MATHEMATICAL MODEL OF A TURBULENT GAS FLOW IN A ZIGZAG CHANNEL

L. P. Kholpanov, B. R. Ismailov, and
N. P. Bolgov

UDC 532.517.4

Many heat- and mass-transfer processes in the chemical industry and adjacent areas proceed under turbulent flow conditions for the medium. Study of the flow in a zigzag channel that is a component element of highly efficient heat- and mass-transfer apparatus is of special interest.

The turbulent flow in a zigzag channel is investigated numerically by the method of the paper [1] in this report. An element of such a channel is represented in Fig. 1 (the shaded area). It is assumed in the mathematical modeling that the flow in the channel is planar and the Kolmogorov–Prandtl hypothesis $\mu_{ef} = C_\mu \rho k^{1/2} \ell$ is valid.

The desired functions ψ, ω, k, ℓ characterizing the turbulent flow in the desired channel are found from the solution of a system of nonlinear partial differential equations of elliptic type, whose general form in a Cartesian coordinate system is the following

$$a_\varphi \left[\frac{\partial}{\partial \xi_1} \left(\varphi \frac{\partial \psi}{\partial \xi_2} \right) - \frac{\partial}{\partial \xi_2} \left(\varphi \frac{\partial \psi}{\partial \xi_1} \right) \right] - \frac{\partial}{\partial \xi_1} \left[b_\varphi \frac{l_2 r}{l_1} \frac{\partial (c_\varphi \varphi)}{\partial \xi_1} \right] - \\ - \frac{\partial}{\partial \xi_2} \left[b_\varphi \frac{l_1 r}{l_2} \frac{\partial (c_\varphi \varphi)}{\partial \xi_2} \right] + l_1 l_2 r d_\varphi = 0. \tag{1}$$

The x coordinate is directed along the flow, and y is transverse to it, i.e., $\xi_1 = x$, $\xi_2 = y$, $\ell_1 = \ell_2 = 1$, $r = 1$. Values of the function a_ϕ, b_ϕ, c_ϕ, d_ϕ, ϕ, in Eq. (1) are represented in the table. The specific equation for each function ψ, ω, k, ℓ is obtained from (1) with the coefficients indicated in the table taken into account.

For the stream function

$$\frac{\partial}{\partial x} \left(\frac{1}{\rho} \frac{\partial \psi}{\partial x} \right) + \frac{\partial}{\partial y} \left(\frac{1}{\rho} \frac{\partial \psi}{\partial y} \right) + \omega = 0, \tag{2}$$

for ρ = const

$$\frac{\partial^2 \psi}{\partial x^2} + \frac{\partial^2 \psi}{\partial y^2} = -\rho \omega. \tag{3}$$

For the vortex intensity

$$\frac{\partial}{\partial x} \left(\omega \frac{\partial \psi}{\partial y} \right) - \frac{\partial}{\partial y} \left(\omega \frac{\partial \psi}{\partial x} \right) - \frac{\partial}{\partial x} \left[\frac{\partial (\mu_{ef} \omega)}{\partial x} \right] - \frac{\partial}{\partial y} \left[\frac{\partial (\mu_{ef} \omega)}{\partial y} \right] - S_\omega = 0 \tag{4}$$

$$(S_\omega = 0 \text{ from } [1]),$$

for $\mu_{ef} \equiv \mu$

$$u \frac{\partial \omega}{\partial x} + v \frac{\partial \omega}{\partial y} = \mu \left(\frac{\partial^2 \omega}{\partial x^2} + \frac{\partial^2 \omega}{\partial y^2} \right). \tag{5}$$

Institute of New Chemical Problems, Academy of Sciences of the USSR, Moscow. Translated from Inzhenerno-Fizicheskii Zhurnal, Vol. 56, No. 6, pp. 910-915, June, 1989. Original article submitted December 2, 1987.

0022-0841/89/5606-0625$12.50

TABLE 1. Values of the Parameters of Equation 1

φ	a_φ	b_φ	c_φ	d_φ
ψ	0	$1/\rho$	1	$-\omega$
ω	1	1	μ_{ef}	$-S_\omega$
k	1	$\Gamma_{k\,ef}$	1	$-S_k$
l	1	$\Gamma_{l\,ef}$	1	$-S_l$

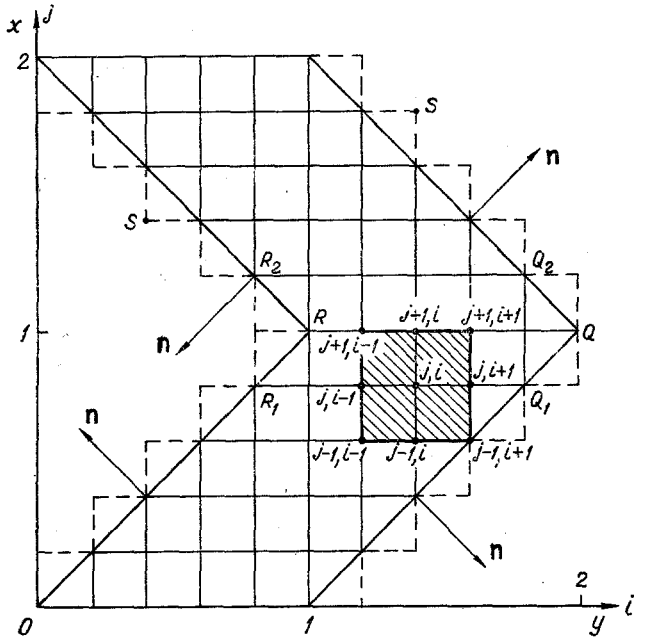

Fig. 1. Network integration domain.

As we see, Eqs. (3) and (5) are the Navier–Stokes equation in stream function-vortex variables for the laminar flow mode.

For the kinetic energy of the turbulent fluctuations

$$\frac{\partial}{\partial x}\left(k\frac{\partial\psi}{\partial y}\right)-\frac{\partial}{\partial y}\left(k\frac{\partial\psi}{\partial x}\right)-\frac{\partial}{\partial x}\left(\mu_{ef}\frac{\partial k}{\partial x}\right)-\frac{\partial}{\partial y}\left(\mu_{ef}\frac{\partial k}{\partial y}\right)-S_k=0. \tag{6}$$

The source term of the turbulent fluctuations can be represented as follows

$$S_k = W_{\text{кас.к}\,t}-D_k. \tag{7}$$

Here

$$W_{\tan\,t}=\mu_t\left[4\left(\frac{\partial^2\psi}{\partial x\partial y}\right)^2+\left(\frac{\partial^2\psi}{\partial y^2}-\frac{\partial^2\psi}{\partial x^2}\right)^2\right],\quad \mu_t=\mu_{ef}-\mu, \tag{8}$$

$$D_k=\rho k^{3/2}l^{-1}C_D, \tag{9}$$

where C_D is a function of the Turbulent Reynolds number. For large numbers Re_t for which the turbulent flow is modelled in the zigzag channel, C_D tends to a constant value.

For the scale of turbulence

$$\frac{\partial}{\partial x}\left(l\frac{\partial\psi}{\partial y}\right)-\frac{\partial}{\partial y}\left(l\frac{\partial\psi}{\partial x}\right)-\frac{\partial}{\partial x}\left(\mu_{ef}\frac{\partial l}{\partial x}\right)-\frac{\partial}{\partial y}\left(\mu_{ef}\frac{\partial l}{\partial y}\right)-S_l=0. \tag{10}$$

The expression for the source number S_ℓ in [1] is obtained in the following form

$$S_l = C_S \rho k^{1/2} - C_B l k^{-1} W_{\text{кас.к}\,t}, \tag{11}$$

where C_S, C_B are functions of Re_t tending asymptotically to constant values as Re_t increases. On the channel surface $S_k = 0$, $S_\ell = 0$.

In the dimensionless variables $x = x^*H$, $\psi = \psi^* H \rho U_0$, $\omega = \omega^* U_0/H$, $k = k^* U^2$, $\mu_{ef} = \mu^*_{ef} H \rho U_0$, $\ell = \ell^* H$, $u = u^* U_0$, $v = v^* U_0$, taking (7), (9), and (11) into account Eqs. (2), (4), (6) and (10) take the form

$$\frac{\partial^2 \psi}{\partial x^2} + \frac{\partial^2 \psi}{\partial y^2} = -\omega, \tag{12}$$

$$\frac{\partial \omega}{\partial x}\frac{\partial \psi}{\partial y} - \frac{\partial \omega}{\partial y}\frac{\partial \psi}{\partial x} - \frac{\partial}{\partial x}\left[\frac{\partial (\mu_{ef}\omega)}{\partial x}\right] - \frac{\partial}{\partial y}\left[\frac{\partial (\mu_{ef}\omega)}{\partial y}\right] = 0, \tag{13}$$

$$\frac{\partial k}{\partial x}\frac{\partial \psi}{\partial y} - \frac{\partial k}{\partial y}\frac{\partial \psi}{\partial x} - \frac{\partial}{\partial x}\left(\mu_{ef}\frac{\partial k}{\partial x}\right) - \frac{\partial}{\partial y}\left(\mu_{ef}\frac{\partial k}{\partial y}\right) =$$

$$= 4\left(\mu_{ef} - \frac{1}{\mathrm{Re}}\right)\left[\left(\frac{\partial^2 \psi}{\partial x \partial y}\right)^2 + \left(\frac{\partial^2 \psi}{\partial x^2} - \frac{\partial^2 \psi}{\partial y^2}\right)^2\right] - C_D k^{3/2} l^{-1}, \tag{14}$$

$$\frac{\partial l}{\partial x}\frac{\partial \psi}{\partial y} - \frac{\partial l}{\partial y}\frac{\partial \psi}{\partial x} - \frac{\partial}{\partial x}\left(\mu_{ef}\frac{\partial l}{\partial x}\right) - \frac{\partial}{\partial y}\left(\mu_{ef}\frac{\partial l}{\partial y}\right) =$$

$$= C_S k^{-1/2} - C_B k^{-1} l \bar{F}, \tag{15}$$

where

$$\bar{F} = \left(\mu_{ef} - \frac{1}{\mathrm{Re}}\right)\left[4\left(\frac{\partial^2 \psi}{\partial x \partial y}\right) + \left(\frac{\partial^2 \psi}{\partial y^2} - \frac{\partial^2 \psi}{\partial x^2}\right)^2\right].$$

A nine-point scheme [1] oriented "against the flow," which assured stability of the computation, was used for the numerical solution of the system (12)-(15). The system of finite-difference equations took the following form

$$\varphi_{j,i} = C_{j+1,i}\varphi_{j+1,i} + C_{j-1,i}\varphi_{j-1,i} + C_{j,i-1}\varphi_{j,i-1} + C_{j,i+1}\varphi_{j,i+1} + D_{j,i}, \tag{16}$$

where

$$C_{j+1,i} = (A_{j+1,i} + B_{j+1,i} C_{\varphi,j+1,i})/\sum_{AB}; \quad C_{j-1,i} = (A_{j-1,i} +$$

$$+ B_{j-1,i} C_{\varphi,j-1,i})/\sum_{AB}; \quad C_{j,i-1} = (A_{j,i-1} + B_{j,i-1} C_{\varphi,j,i-1})/\sum_{AB};$$

$$C_{j,i+1} = (A_{j,i+1} + B_{j,i+1} C_{\varphi,j,i+1})/\sum_{AB}; \tag{17}$$

$$A_{j+1,i} = \frac{a_{\varphi,j,i}}{8}\left[(\psi_{j+1,i} + \psi_{j,i+1} - \psi_{j+1,i+1} - \psi_{j,i-1}) + |Z_1|\right];$$

$$A_{j-1,i} = \frac{a_{\varphi,j,i}}{8}\left[(\psi_{j-1,i-1} + \psi_{j,i-1} - \psi_{j-1,i+1} - \psi_{j,i+1}) + |Z_2|\right]; \tag{18}$$

$$A_{j,i-1} = \frac{a_{\varphi,j,i}}{8}\left[(\psi_{j+1,i-1} + \psi_{j+1,i} - \psi_{j-1,i-1} - \psi_{j-1,i}) + |Z_3|\right];$$

$$A_{j,i+1} = \frac{a_{\varphi,j,i}}{8}\left[(\psi_{j-1,i+1} + \psi_{j-1,i} - \psi_{j+1,i+1} - \psi_{j+1,i}) + |Z_4|\right];$$

$$B_{j+1,i} = (b_{\varphi,j+1,i} + b_{\varphi,j,i})/2; \quad B_{j-1,i} = (b_{\varphi,j-1,i} + b_{\varphi,j,i})/2;$$
$$B_{j,i-1} = (b_{\varphi,j,i-1} + b_{\varphi,j,i})/2; \quad B_{j,i+1} = (b_{\varphi,j,i+1} + b_{\varphi,j,i})/2; \tag{19}$$

$$\sum_{AB} = A_{j+1,i} + A_{j-1,i} + A_{j,i-1} + A_{j,i+1} + C_{\varphi,j,i}(B_{j+1,i} + B_{j-1,i} + B_{j,i-1} + B_{j,i+1}); \tag{20}$$

$$D_{j,i} = -d_{\varphi,j,i} V_{j,i} / \sum_{AB}, \quad V_{j,i} = \frac{1}{4}(x_{j+1} - x_{j-1})(y_{i+1} - y_{i-1});$$

$|Z_m|$ is the absolute value of the circular bracket, m = 1, 2, 3, 4.

The second-order derivatives were replaced by finite-differences by the formulas

$$\left(\frac{\partial^2\psi}{\partial x \partial y}\right)_{j,i} = \frac{\psi_{j+1,i+1} - \psi_{j+1,i-1} - \psi_{j-1,i+1} + \psi_{j-1,i-1}}{4h^2},$$
$$\left(\frac{\partial^2\psi}{\partial x^2}\right)_{j,i} = \frac{\psi_{j+1,i} - 2\psi_{j,i} + \psi_{j-1,i}}{h^2},$$
$$\left(\frac{\partial^2\psi}{\partial y^2}\right)_{j,i} = \frac{\psi_{j,i+1} - 2\psi_{j,i} + \psi_{j,i-1}}{h^2}.$$

The dynamic boundary conditions on the solid bounary are given in the form ψ = const, $\partial\psi/\partial n = 0$ during solution of the problems in the stream function-cortex system. Therefore, the boundary conditions are not given for the vortices, which is one of the characteristic singularities of the solution of the Navier–Stokes equations in the stream function-vortex system. Apropos solvability of the boundary conditions for the vortex, sufficiently many approaches exist [2].

The following boundary condition for the vortex is selected in this report

$$\psi_{ef} - \psi_{gr} = -\left[\frac{1}{6}\left(\frac{\partial\omega}{\partial n}\right)_{gr} n^3 + \frac{\omega_{gr}}{2} n^2\right], \tag{21}$$

where the gradient of the vortex along the normal $(\partial\omega/\partial n)_{gr}$ is taken with channel geometry taken into account, i.e., is calculated from the formula

$$\partial\omega/\partial n = \partial\omega/\partial x \sin(n, x) + \partial\omega/\partial y \cos(n, y),$$

where n is the distance between the boundary surface and the nearest internal node.

Linear extrapolation is used in approximating nodes outside the contours S and the derivatives at the pionts Q and R are found as the mean values in adjacent boundary points (Fig. 1).

The turbulence constants in the computational formulas are taken in conformity with values known in the literature: $C_\mu = 0.1$, $C_D = 0.055$, $C_S = 0.0397$, $C_B = 1.05$. It should be noted that the variation of certain constants (C_μ, C_B) yielded no substantial changes in the final results.

The sequence for computing the stream function, vortex intensity, kinetic energy, and scale of turbulence was the following.

1. Using (17)-(20) by means of given values of ψ at the inner nodes values were found for the coefficients $A_{j,i}$, $B_{j,i}$, $C_{j,i}$, $D_{j,i}$. Used for the boundary nodes in the calculation of these coefficients is (21), which, taking channel geometry into account, took the following values (for instance, for the first half of the left boundary)

$$\omega_{j,i} = -\frac{3(\psi_{j-1,j+1} - \psi_{j,i})}{5h^2} + \frac{\omega_{j-1,i} + \omega_{j,i+1}}{5}. \tag{22}$$

The structure of the formulas is analogous to (22) for the remaining sections of the channel boundary.

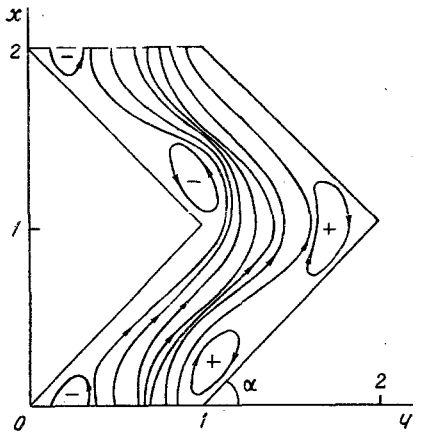

Fig. 2

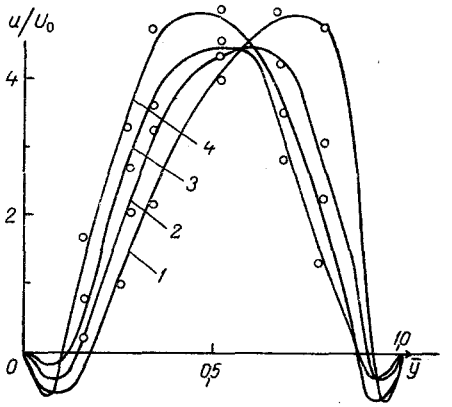

Fig. 3

Fig. 2. Isolations of the stream function in a zigzag channel (a = 110 mm, H = a, α = 45°) for Re = $4 \cdot 10^4$.

Fig. 3. Change in vertical velocity component in different channel sections (Re = $4 \cdot 10^4$) at different heights: 1) x = 0, 2) 0.2, 3) 0.4, 4) 0.8 ($\bar{y}$ is the distance from the left boundary of the channel); the points are test data.

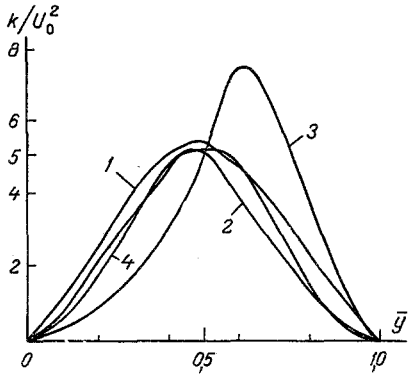

Fig. 4

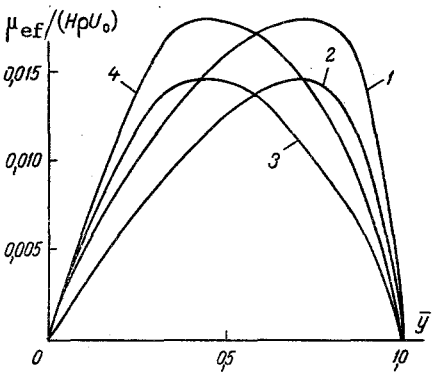

Fig. 5

Fig. 4. Kinetic energy distribution of turbulent fluctuations over the channel section (Re = $4 \cdot 10^4$) at different heights: 1) x = 0.2, 2) 0.4, 3) 0.8, 4) 1.

Fig. 5. Effective viscosity distribution over the channel section (Re = $4 \cdot 10^4$) at different heights: 1) x = 0.1, 2) 0.3, 3) 0.8, 4) 1.

2. The desired function $\phi = \psi, \omega, k, \ell$ is calculated.

3. The achievement of the accuracy of solving the system of equations (12)-(15) is verified: $\max_{\varphi} \{|\varphi^{(2)} - \varphi^{(1)}| / |\varphi^{(2)}|\} < \varepsilon$.

4. The computation is repeated, starting from No. 1 when the conditions for achieving the required accuracy are not satisfied.

The velocity profile, pressure drip in the channel, effective viscosity, and other dynamic quantities are determined from the functions $\phi = \psi, \omega, k, \ell$ found.

The computation is performed in a broad Reynolds number range (Re = $2 \cdot 10^3$-$4 \cdot 10^4$). The characteristic flow pattern is represented in Fig. 2. As follows from the computation, vortices are formed on both sides of the channel. The stream function isolines are compressed behind the acute angle of channel rotation, which indicates the formation of a domain with predominance of the vertical velocity component (for example, for u_0 = 5 m/sec, u_0 = 25-30 m/sec). This circumstance contributes to acceleration of the process when using a vertical zigzag channel as contact unit in heat and mass transfer processes. Stagnant zones are formed at the right wall in the channel rotation domain, which reduces the heat and mass

transfer efficiency in this area. This is also confirmed by the behavior of the other dynamic flow characteristics represented in Figs. 3-5.

Results of an experimental measurement of the vertical velocity component at different channel sections are represented in Fig. 3. Data on the velocity distribution are obtained by using a cylindrical probe. The measurements are performed by the method described in [3].

The approach examined for describing turbulent incompressible fluid flow affords the possibility of obtaining total hydrodynamic information about incompressible fluid flow in not only zigzag channels but also in channels with any geometry (for instance, wavy channels) whose utilization will permit significant intensification of heat and mass transfer process.

NOTATION

μ, μ_{ef}, molecular and effective turbulent viscosity; C_μ, a constant; k, kinetic energy of turbulent fluctuations; ℓ, local scale of turbulence; ψ, stream function; ω, vorticity; Γ_{keV}, transfer coefficient of the kinetic energy of fluctuating motion k; $\Gamma_{\zeta eV}$, transfer coefficient of a vortex with scale; $\sigma_k = \mu_{ef}/\Gamma_{keV}$, $\sigma_\ell = \mu_{ef}/\Gamma_{\zeta ef}$; S_k, source term of turbulent fluctuations; $W_{tan\ t}$, kinetic energy produced by turbulent tangential stresses per unit time; D_k, energy dissipation per unit volume comprising the negative part of the energy source; $Re_t = \rho k^{1/2} \ell \mu^{-1}$, turbulent Reynolds number; $Re = U_0 \rho H/\mu$, Reynolds number computed according to the mean flow rate; H, channel width, U_0, mean mass flow rate; ψ_{gr}, ψ_{vn}, stream function values at the boundary and adjacent nodes; $h_x = h_y = h$, network spacing.

LITERATURE CITED

1. A. D. Gosmen, V. M. Pan, A. K. Ranchel, et al., Numerical Methods of Investigating Viscous Fluid Flow [in Russian], Moscow (1972).
2. V. S. Avduevskii (ed.), Mathematical Modeling of Convective Heat and Mass Transfer on the Basis of the Navier–Stokes Equations [in Russian], Moscow (1987).
3. I. L. Povkh, Technical Hydromechanics [in Russian], Leningrad (1969).